JOURNAL OF GEOPHYSICAL RESEARCH, VOL. 104, NO. C9, PAGES 21,063–21,082, SEPTEMBER 15, 1999

Intermediate water in the Brazil-Malvinas Confluence Zone: A Lagrangian view

Olaf Boebel,[1] Claudia Schmid,[2] Guillermo Podestá,[3] and Walter Zenk[2]

Abstract. The subsurface flow within the subantarctic and subtropical regions around the Brazil-Malvinas (Falkland) Confluence Zone is studied, using daily hydrographic and kinematic data from four subsurface floats and a hydrographic section parallel to the South American shelf. The float trajectories are mapped against sea surface flow patterns as visible in concurrent satellite sea surface temperature (SST) images, with focus on the November 1994 and October/November 1995 periods. The unprecedented employment of Lagrangian θ-S diagrams enables us to trace the advection of patches of fresh Antarctic Intermediate Water (AAIW) from the Confluence Zone into the subtropical region. The fresh AAIW consists of a mixture of subtropical AAIW and Malvinas Current core water. Within the subtropical gyre, these patches are discernible for extended periods and drift over long distances, reaching north to 34°S and east to 40°W. The cross-frontal migration of quasi-isobaric floats across the Confluence Zone from the subtropical to the subantarctic environment is observed on three occasions. The reverse process, float migration from a subpolar to a subtropical environment was observed once. These events were located near 40°S, 50°W, the site of a reoccurring cold core feature. Subsurface float and SST data comparison reveals similarities with analogous observations made in the Gulf Stream [*Rossby*, 1996] where cross-frontal processes were observed close to meander crests. The limited number of floats of this study and the complex structure of the Brazil-Malvinas Confluence Zone, however, restricts the analysis to a description of two events.

1. Introduction

1.1. Brazil-Malvinas (Falkland) Confluence Zone

The total Malvinas (Falkland) Current transport (see Figure 1 for the location of named features) was recently modified toward significantly higher values. Contrary to earlier estimates [*Confluence Principal Investigators*, 1990; *Gordon and Greengrove*, 1986; *Piola and Bianchi*, 1990] of 10–15 Sv (1 Sv = 10^6 m^3 s^{-1}), the along-shelf transport is now believed to be of the order of 70–80 Sv [*Peterson*, 1990, 1992; *Peterson et al.*, 1996]. This is largely due to a strong barotropic component, which was revealed by direct current measurements. Surface drifters, drogued at 100 m depth, indicate near-surface speeds of up to 140 cm s^{-1} [*Peterson et al.*, 1996] and Autonomous Lagrangian Circulation Explorer (ALACE) floats [*Davis et al.*, 1992] at intermediate depth unveil an along-shelf flow of 30–40 cm s^{-1} [*Davis et al.*, 1996] in the Malvinas Current core. Estimates of the abyssal depth flow are of the order of 10–30 cm s^{-1} [*Peterson et al.*, 1996].

Similar findings have been made for the Brazil Current (BC) south of the Santos Bifurcation (O. Boebel et al., manuscript in preparation, 1998). Near 37°S, the transport of the southern Brazil Current has increased to ≈75 Sv [*Peterson*, 1990; *Zemba and McCartney*, 1988] by vertical enhancement through the southward flow at intermediate and greater depth. It is arguable if these vertical extensions of the Brazil Current should be included in the Brazil Current transport estimates. From a kinematic point of view, there is no level of zero velocity between the sea surface and the bottom, suggesting that the whole water column could be treated as a single current. From a hydrographic point of view, however, the addition of Antarctic Intermediate Water (AAIW) and North Atlantic Deep Water to the Brazil Current does not contribute to additional transport of South Atlantic Central Water to the southwest, and one may wish tc exclude it from the BC transport proper (see *Peterson and Stramma* [1991] or *Garzoli* [1993] for detailed discussions of transport estimates). To our knowledge, no direct Eulerian velocity measurements have been published from this southernmost part of the Brazil Current [*Müller et al.*, 1998], but Lagrangian measurements indicate a mean southwestward, along-shelf flow of order 6 cm s^{-1} at intermediate depth (O. Boebel et al., manuscript in preparation, 1998) with peak speeds of 20 cm s^{-1}.

When the Malvinas and Brazil Currents collide between 35°S and 40°S [*Garzoli*, 1993; *Garzoli and Giulivi*, 1994] off the Argentinean and Uruguayan coasts, they are deflected away from the western boundary toward the open ocean. The northern collision positions are more likely to be occupied during austral winter [*Garzoli and Garraffo*, 1989; *Olson et al.*, 1988; *Peterson and Stramma*, 1991], but strong interannual variability, probably related to wind field variations [*Garzoli and Giulivi*, 1994], hinders reliable predictions. The mean separation point of the Brazil Current from the continental shelf is near 36° [*Olson et al.*, 1988] and varies between 33°S and 38°S [*Peterson and Stramma*, 1991], while the Malvinas Current separates in the average farther south near 39°S [*Olson et al.*, 1988].

Subsequently, the Brazil Current extension and the return flow of the Malvinas Current (MC) flow side by side toward the

[1]Department of Oceanography, University of Cape Town, Rondebosch, South Africa.
[2]Institut für Meereskunde, Universität Kiel, Kiel, Germany.
[3]Rosenstiel School of Marine and Atmospheric Sciences, University of Miami, Miami, Florida.

Paper number 1999JC900059.
0148-0227/99/1999JC900059$09.00

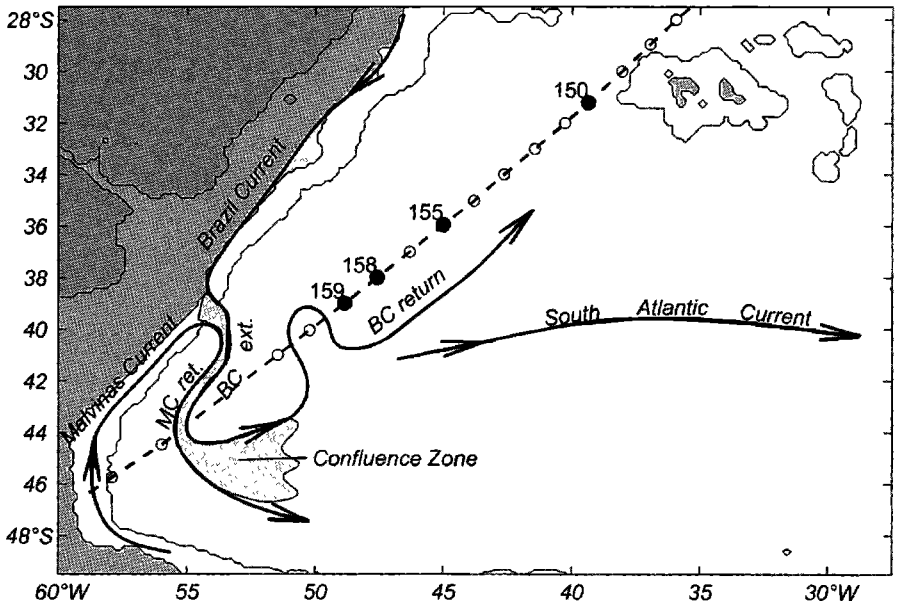

Figure 1. Map of the area of investigation, indicating major oceanographic features and their names [after *Peterson and Stramma*, 1991; *Confluence Principal Investigators*, 1990; *Gordon*, 1989; etc.]. Indicated features are the Malvinas Current, the Malvinas Current return (MC ret.), the Brazil Current, the Brazil Current extension (BC ext.), the Brazil Current return (BC return) and the South Atlantic Current. The Malvinas Current and its return are associated with the Subantarctic Front (not shown), whereas the path of the Brazil Current and its extension is a proxy for the Brazil Current Front. The Confluence Zone describes the area of close proximity of the Subantarctic and Brazil Current Front. Here, and in other maps, the continent and the shelf up to the 1000-m isobath are indicated by dark (yellow) and light (green) hatching; the 3000-m isobath is only indicated by a line. The cruise track of *Polarstern* cruise Antarctic (ANT) XII, leg 1 is plotted as dashed line. Positions of conductivity-temperature-depth (CTD) stations (Table 1) are marked by circles or dots when a float was launched at the same site.

south-southeast and away from the coast (Figure 1). The combined flow of the two currents causes a strong thermohaline frontal region (Plate 1), commonly known as Brazil-Malvinas Confluence Zone [*Confluence Principal Investigators*, 1990; *Gordon and Greengrove*, 1986]. This zone is characterized by highly variable sea surface temperature and salinity contrasts. The warm Brazil Current extension reaches latitudes of at least 38°S [*Confluence Principal Investigators*, 1990; *Legeckis and Gordon*, 1982; *Roden*, 1986] before it retroflects back north, but its southernmost branch may extend as far south as 44°S.

During the interaction between the Brazil Current extension and Malvinas Current return, cross-frontal exchanges are expected to occur at all depths [*Gordon*, 1981]. Near the sea surface, strong eddy variability is observed in the Confluence Zone, and patches of warm water are found south of the Subantarctic Front (SAF) [*Roden*, 1986], as well as cold water north of the Brazil Current Front (BCF) [*Gordon*, 1989]. At intermediate depths the low-salinity Antarctic Intermediate Water layer (Plate 2b) is characterized by strong horizontal density gradients across the Confluence Zone. The extension of the large surface variability throughout the upper 1000 m has been reported by *Garzoli* [1993], but details of the underlying mechanisms still remain unobserved and unquantified [*Peterson and Stramma*, 1991].

1.2. Antarctic Intermediate Water in the Confluence Zone

Representative isopycnals (27.05–27.2σ_θ) of the AAIW core layer [*Bianchi et al.*, 1993; *Piola and Gordon*, 1989] are found at 800–900 m depth north of the Confluence Zone and at 200–400 m depth to the south of it. Fresh AAIW from the subantarctic region is thought to flow northward and eastward across the Confluence Zone while sinking along these isopycnals and to enter the subtropical South Atlantic [*Peterson and Whitworth*, 1989], but details of this process are poorly understood.

Once injected into the subtropical gyre, the AAIW is carried east with the South Atlantic Current (SAC) [*Stramma and Peterson*, 1990] across the South Atlantic. East of the Mid-Atlantic-Ridge, the water takes a northward route until it is deflected back west near 30°S. The Subtropical Gyre Return Current [*Boebel et al.*, 1999] then carries the AAIW back to the western boundary where the flow bifurcates near the Santos Bifurcation. Some parts form a narrow northward intermediate western boundary current, whereas about three quarters [*Schmid*, 1998] are deflected to the south, joining the southwestward flow of the near-surface Brazil Current and feeding back into the Confluence Zone. Here the cycle is closed and recirculated AAIW, which increased in salinity during its transatlantic excursion, again interacts with fresh and new Antarctic Intermediate Water from the subantarctic regions [*Gordon*, 1981; *Maamaatuaiahutapu et al.*, 1994].

The discussion on the actual formation mechanism of fresh Antarctic Intermediate Water has focused on three possibilities: (1) the mixing of Antarctic Surface and subsurface water with Subantarctic Surface Water [*Deacon*, 1933; *Wüst*, 1935] (2) the freshening of Subantarctic Mode Water (SAMW) by air-sea interaction while traveling from the SAMW formation site in the eastern South Pacific with the Malvinas Current to the Confluence Zone [*McCartney*, 1977], and (3) a synthesis

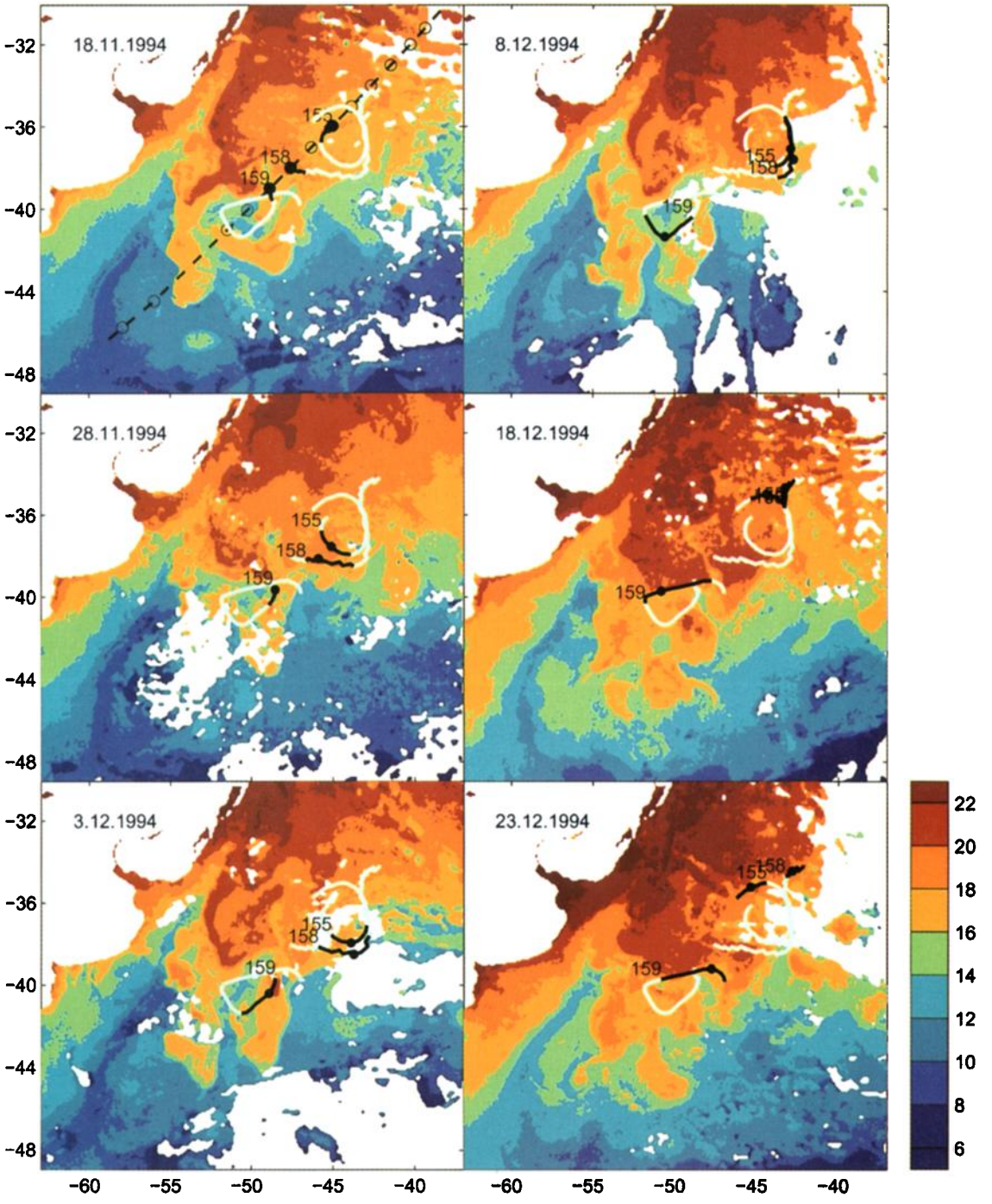

Plate 1. Satellite sea surface temperature (SST) of the Confluence Zone between November 18, 1994, and December 23, 1994. The SST images are 5-day maximum temperature composites, centered around the day indicated in the upper left corner in day-month-year format. Float trajectory segments (black) spanning 10 days are centered around the same date (with the corresponding float position indicated by a solid dot). The float number is indicated next to the segment start. As guide to the eye, gray float trajectory segments span the total period (November 18 to December 23, 1994) covered by this figure.

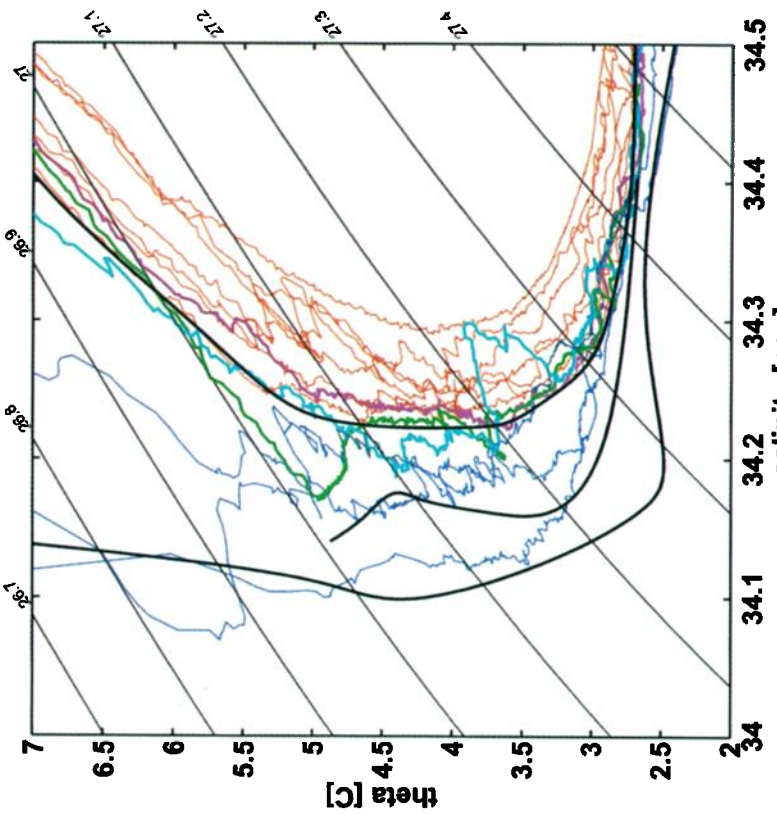

Plate 3. Potential temperature-salinity diagram of selected CTD stations (Table 1). Stations within the subtropical regime are red, and those within the subantarctic regime are blue. Data from stations 35, 38, and 41 are magenta, green, and cyan, respectively. The lower salinities of the subtropical regime are delimited by the black curve on the right. Potential temperature-salinity data from the Malvinas Current core is indicated by the black curve in the middle [after *Piola and Gordon*, 1989, Figure 5]. Data from within the cyclonic trough of the Malvinas current are indicated by the black curve on the left [after *Piola and Gordon*, 1989, Figure 7].

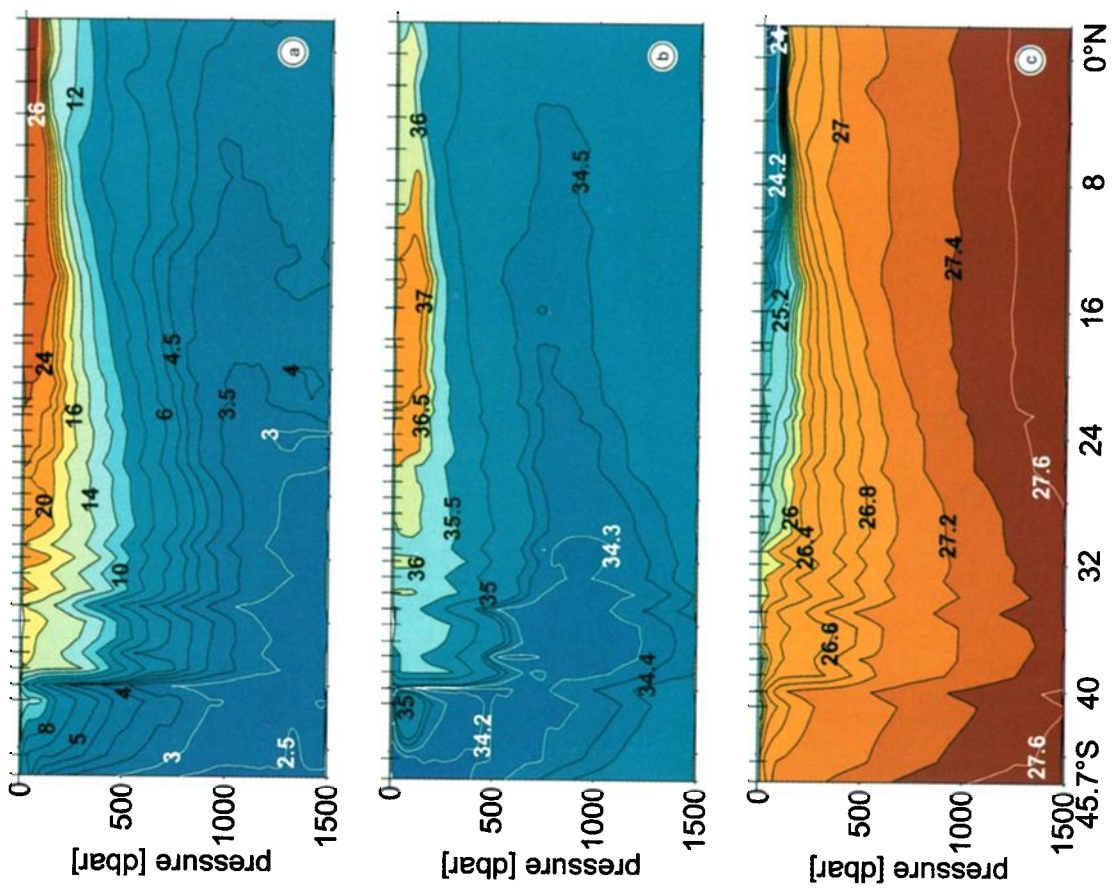

Plate 2. (a) Potential temperature, (b) salinity, and (c) potential density, sections along the track of *Polarstern* cruise ANT XII, leg 1. See Table 1 and Figure 1 for the location of the section.

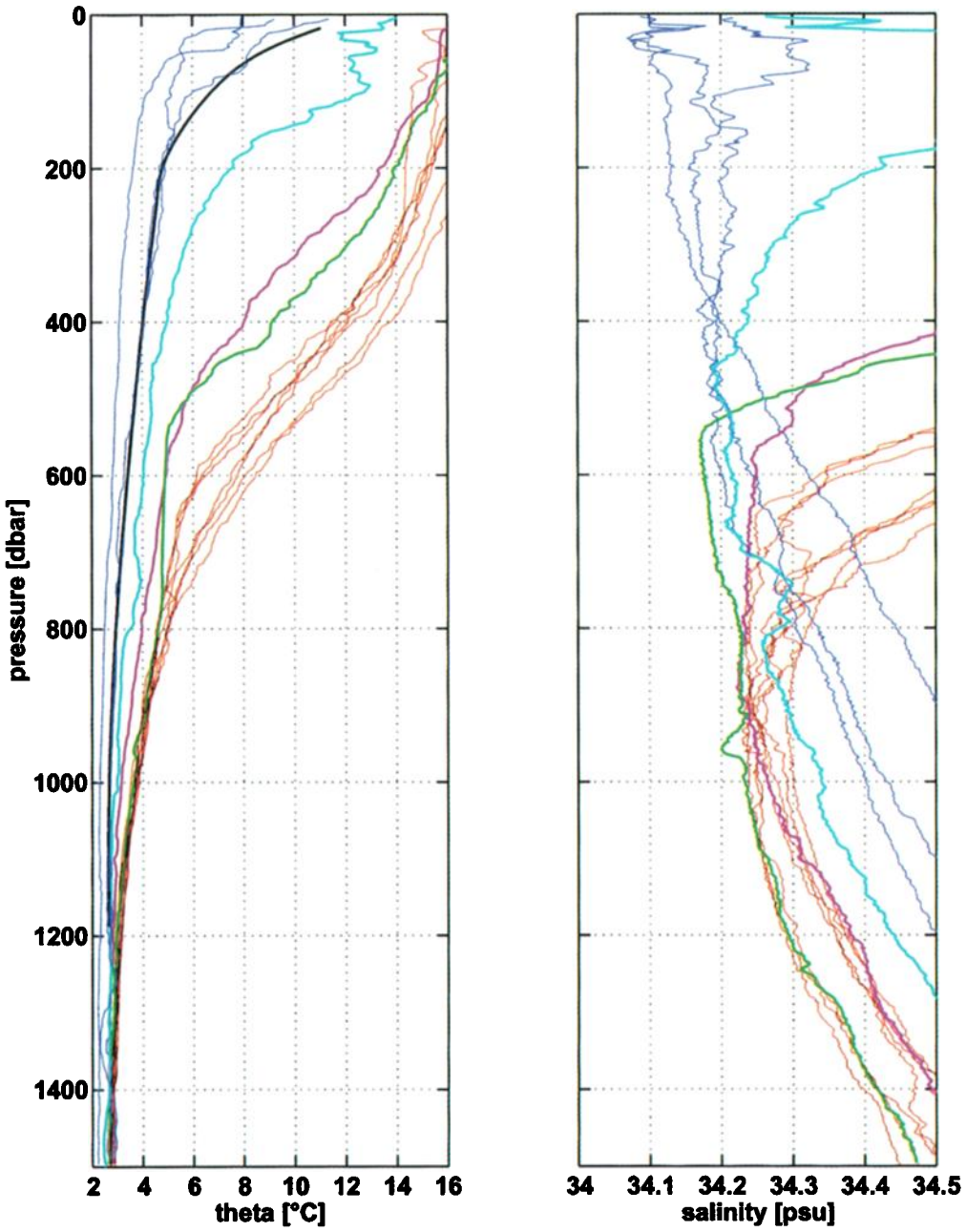

Plate 4. (left) Vertical potential temperature and (right) salinity profiles of selected CTD stations (Table 1). Color coding as in Plate 3 and Table 1.

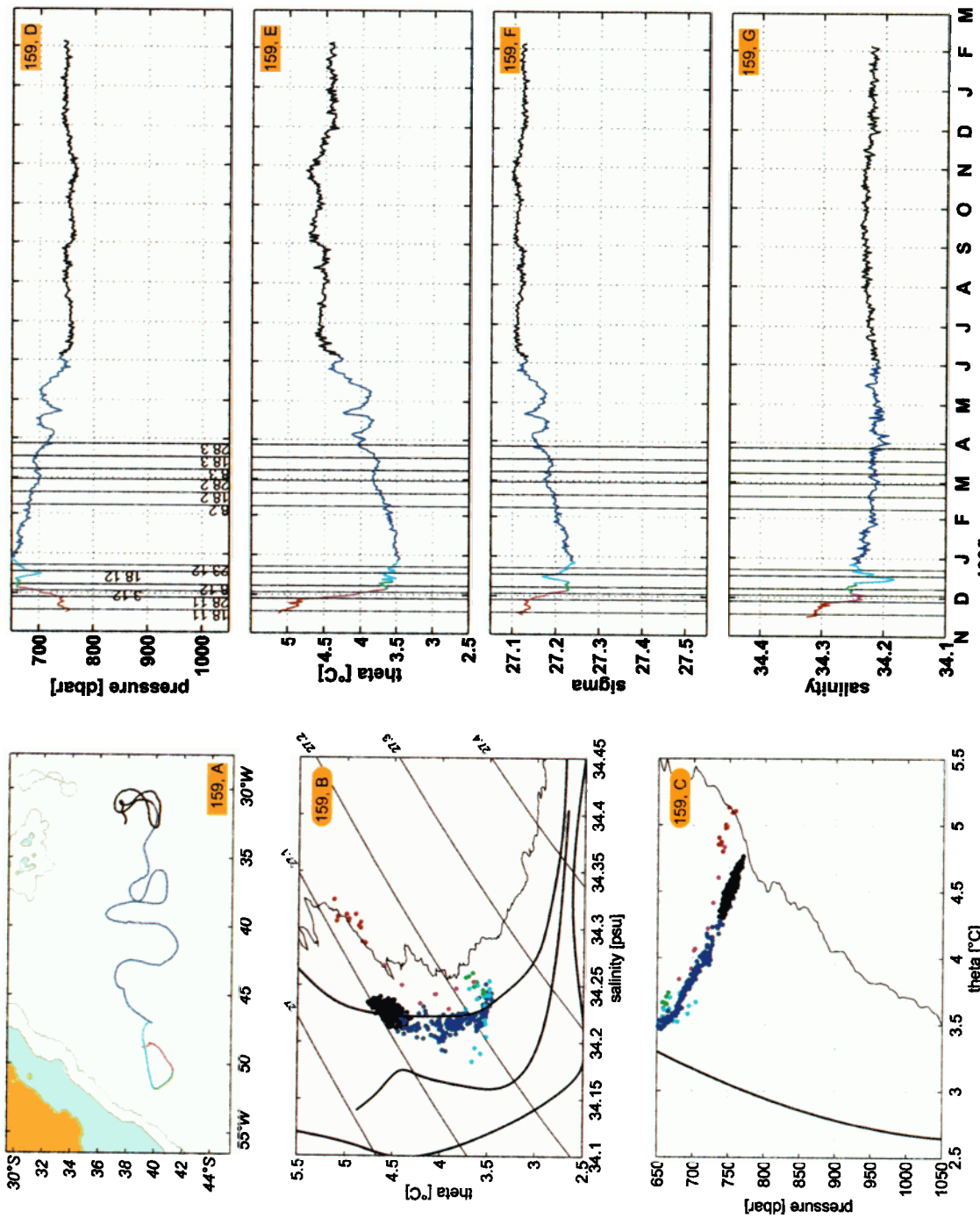

Plate 5. Float 159. (a) Full trajectory between launch and surface position. The float surfaced on schedule after nominal 15 months. (b) Lagrangian potential temperature-salinity diagram (dots). The boundaries between different water regimes are given as solid curves (compare Plate 3). The CTD cast taken prior to the float seeding is depicted as thin curve. (c) Pressure-potential temperature diagram. (d) Pressure, (e) potential temperature, (f) potential density, and (g) salinity time series. Vertical lines refer to times at which satellite images are discussed (Plates 1 and 6).

Table 1. List of CTD Stations and Float Launch Positions

Date 1994	Latitude, °S	Longitude, °W	Station	Color Code	Float	Feature
Nov. 12	31°12′	39°22′	31	red	150	
	32°00′	40°16′	32	red		
	33°00′	41°27′	33	red		
Nov. 13	34°00′	42°39′	34	red		
	35°01′	43°51′	35	magenta		C-α
	35°57′	45°01′	36	red	155	
Nov. 14	37°00′	46°19′	37	red		
	38°00′	47°35′	38	green	158	C-β
Nov. 15	39°00′	48°51′	39	red	159	
	40°03′	50°13′	40	blue		C-γ
Nov. 16	41°00′	51°28′	41	cyan		A-α
Nov. 17	44°28′	55°59′	42	blue		
Nov. 18	45°45′	57°55′	43	blue		

See Figure 1 for a graphic representation. The indicated colors are used in Plates 3 and 4.

hereof which requires an Antarctic water mass component in the formation of AAIW from SAMW [*Piola and Gordon*, 1989]. The latter two mechanisms favor the Confluence Zone as the primary site of injection of fresh AAIW into the subtropical gyre, since it is here where the Malvinas Current first encounters the subtropical water regime. Recent studies, however, have revealed exchanges between the South Atlantic and Antarctic Circumpolar Currents over much of the South Atlantic's longitudinal extend (O. Boebel et al., manuscript in preparation, 1998) and also in the Crozet Basin [*Park and Gamberoni*, 1997]. This might necessitate reconsideration of the possibility of a direct exchange across the whole circumference of the Southern Ocean northern boundary.

Nevertheless, in this study we focus on exchange processes within the Confluence Zone and the various water types involved. In a detailed investigation of the regions hydrography, *Piola and Gordon* [1989] distinguish among three different hydrographic regimes of potential temperature-salinity properties: (1) the subtropical regime, (2) the Malvinas Current core, and (3) the cyclonic trough formed by the Malvinas Current and its return. They suggest that the water type found within the Confluence Zone is formed by mixing water of subtropical origin and water from the Malvinas Current core. The latter water type is derived from the Subantarctic Zone (the region between the Subtropical and the Subantarctic Front) of the northern Drake Passage and has been freshened during its northward passage through precipitation as well as mixing with the fresher water that originated from the Polar Frontal Zone [*Piola and Gordon*, 1989] (the region between the Subantarctic and the Polar Front). Polar Frontal Zone water itself is "folded" into the interior of the cyclonic trough but does not subduct northward underneath the subtropical regime [*Piola and Gordon*, 1989].

The interior trough regime is marked by the lowest subsurface salinities observed. At relatively shallow depths of 200 m, *Piola and Gordon* [1989] noted salinities as low as 34.1 near the

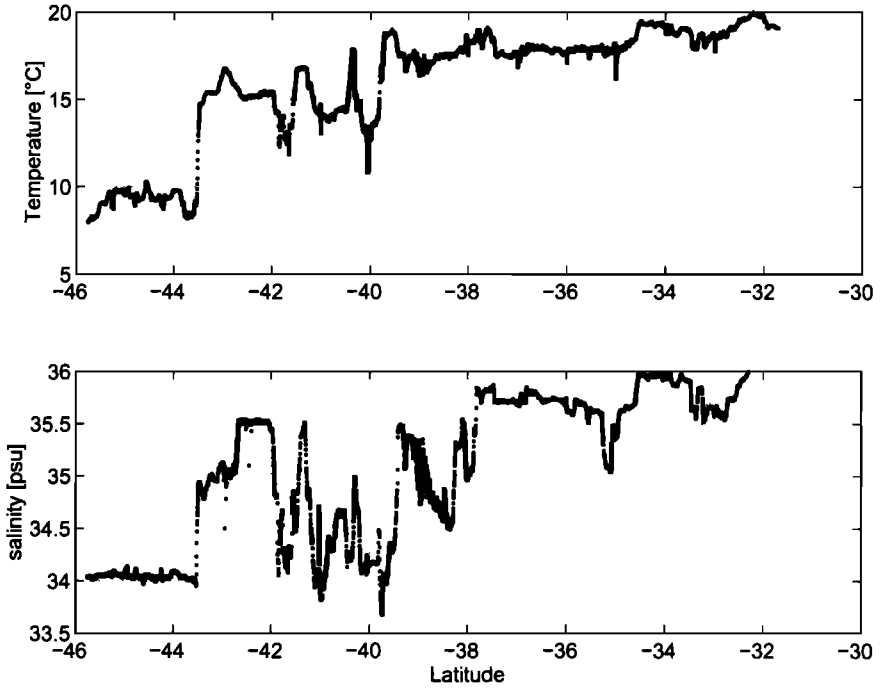

Figure 2. Thermosalinograph data along the cruise track (Figure 1 and Plate 1) between 32°S and 46°S.

$27.05\sigma_\theta$ isopycnal. The θ-S relation characteristic for this regime is indicated by the black curve to the left in Plate 3 [after *Piola and Gordon*, 1989, Figure 7]. The interior trough water assists in freshening water of subantarctic origin that flows along the anticyclonic side of the Malvinas Current core. When the Malvinas Current core water reaches the Confluence Zone and detaches from the western boundary, it has freshened with respect to its source water by 0.04 to $S_{min} = 34.16$ [*Piola and Gordon*, 1989]. It is this Malvinas Current core water (black curve in the middle in Plate 3 [after *Piola and Gordon*, 1989, Figure 5]) that interacts directly with recirculated subtropical AAIW within the Confluence Zone [*Gordon*, 1981]. Mixtures of these water types, located between black curves in the middle and left in Plate 3, will be called Confluence Zone Water hereinafter, or occasionally "subantarctic" water for brevity.

The subtropical regime is characterized by a salinity minimum at $S \geq 34.22$ (Plate 3, black curve on the right). A limit of 34.20 [*Piola and Gordon*, 1989, Figure 9] or 34.21 [*Gordon*, 1989, Figure 11] could be chosen as the lowest possible value of salinity, but stations that reach this limit already show interleaving, which indicates recent mixing processes with fresher water. At higher densities ($\sigma_\theta > 27.3$) the distinction between the various water types is difficult in the θ-S diagrams. However, vertical potential temperature profiles (Plate 4, left) distinguish between the subantarctic/subtropical and subpolar regime by means of the low temperatures found at significantly shallower depths south of the Subantarctic Front than north of it (black curve) [*Ikeda et al.*, 1989].

In section 2.1, we describe the hydrographic data and relate our findings to the frontal and water mass definitions from the literature. This description is extended and enhanced in section 2.2 by a discussion of the sea surface temperature data from November 1994. In section 3, for each float individually, the description of the trajectory is accompanied by a discussion of the corresponding Lagrangian hydrographic data (including derived float density and salinity). This enables us to identify the type of water tagged by selected trajectory segments and to trace the flow of fresh AAIW from the Confluence Zone into the subtropical gyre interior. We also combine the float data with satellite sea surface temperature to relate trajectory segments to surface features. Section 4 discusses our data with regard to the advection, lifetime, and origin of low-salinity patches within the subtropical gyre. A brief discussion of the behavior of quasi-isobaric floats and recent improvements in the method of salinity derivation from float data is given in Appendices A and B, respectively.

2. Confluence Zone in November 1994

2.1. Hydrography

The quasi-isobaric RAFOS floats [*Rossby et al.*, 1986] described in this study (Table 1) were launched from aboard R/V *Polarstern* in November 1994 [*Boebel and Schmid*, 1995]. Each float setting was preceded by a conductivity-temperature-depth (CTD) cast, which was used to determine the physical parameters at the salinity minimum of the AAIW. The floats were ballasted in situ to make them neutrally buoyant close to the depth of the local salinity minimum. The cruise resulted in a slanted section through the eastern region of the Confluence Zone (Figure 1), reaching from the interior Subtropical Gyre into the cyclonic trough formed by the Malvinas Current and its return (Plate 1, top left).

The salinity minimum is observed between 700 and 900 m north of 30°S (Plate 2b). South of this latitude, an undulating isopleth structure is observed. Most pronounced is the doming of the isopleths near at 35°S and 38°S. Geostrophic velocity estimates from the resulting density field (Plate 2c) indicate the presence of cyclonic flow patterns, which we name C-α (35°S) and C-β (38°S), with the C indicating the cyclonic character. The doming isopleths of C-β did not reach the sea surface, whereas the 17°C isotherm (Plate 2a) did nearly crop out over C-α. The potential temperature-salinity diagram at C-α (Plate 3, magenta curve) does not differ from the typical shape found at subtropical stations, but at C-β (Plate 3, green curve), significant freshening is observed between 27.0 and $27.1\sigma_\theta$ and near the $27.2\sigma_\theta$ surfaces.

Between 39°S and 40°S, isotherms in the 12°C–16°C temperature range crop out, and the depth of the salinity minimum changes from 950 to 700 dbar (Plate 2b). These features comply with the description of the climatological mean of the Brazil Current Front (BCF) as given by *Roden* [1986]. Other BCF identifying criteria [*Gordon and Molinelli*, 1982] such as the positioning of the 10°C isotherm and the 34.8 isohaline between 300 and 500 m are met as well.

South of the front the isopleths descend again. The corresponding density field between 39°S and 41°S indicates a cyclonic circulation C-γ superposed to the BCF and an anticyclonic feature A-α to the south of it near 41°S. The higher surface temperatures (>12°C) and increased subsurface salinity suggest that subtropical water is located near 41°S, 51.5°W, south of the presumed Brazil Current Front. This is confirmed by the θ-S data of station 41 (Plate 3, cyan), which is situated closely to the delimiting curve of the subtropical regime (Plate 3, black curve on the right). The interleaving structure, however, indicates that mixing between subtropical water, prevailing below 27.2 σ_θ, and subantarctic water, predominant between 27.1 and 27.2 σ_θ, has occurred. At the sea surface, salinities lower than typical for subtropical water are observed at station 41 (Plate 4, right) which might be due to freshwater from the Rio de la Plata outflow. In fact, the sea surface properties (14°C, 34.26 psu) are situated amidst the cloud of "warmed Malvinas/River Plume Water" as presented by *Gordon* [1989, Figure 4].

Owing to a large gap of CTD stations between 41°S and 44.5°S, the Subantarctic Front location is extracted from the hull-mounted thermosalinograph data (Figure 2). Near 43.5°S a sharp drop in the sea surface temperature from above 15°C to below 10°C and an associated freshening from around 34.9 to 34.0 psu was recorded. The outcropping of the 10°C isotherm and the 34.8 isohaline are characteristic features for the climatological mean of the Subantarctic Front [*Roden*, 1986].

2.2. Sea Surface Temperature

On November 18, 1994, the sea surface temperature (SST) distribution (Plate 1, top left, labeled 18.11.1994) shows warm water (16°C–18°C, yellow) of the Brazil Current extension [*Olson et al.*, 1988] to extend beyond 44°S before it retroflected toward the northeast. The Malvinas Current return, along the cold side of the 14°C isotherm, flows directly to the south of the Brazil Current extension before it detached near 52°W and continued in several large meanders. We are aware that the given SST proxies for the Brazil Current extension and Malvinas Current return are ambiguous and differ from those given by other authors due to the seasonal variation in the SST [*Podestá et al.*, 1991; *Provost et al.*, 1992]. An alternative approach, the use the maximum SST gradients as proxies [*Olson*

et al., 1988], however, is consistent with our present choice due to a SST gradient of >4°C across the front as selected here.

The SST distribution along the ship's track (dashed line in Plate 1) is confirmed in detail by the thermosalinograph record (Figure 2). In particular, the position of the rapid thermosalinograph temperature transition from above 15°C to below 10°C, which we used to identify the SAF near 43.5°S, coincides with the intersection of the ships track and the location of the Malvinas Current return from the SST image (yellow to blue transition, Plate 1, November 18).

Near 40°S, 50°W a plume of cold (12°C–14°C, cyan) water was observed until December 8, 1994 (Plate 1). The warm northward Brazil Current return appears to entrain this incoherent patch of cold subantarctic water. The cold water plume was detached from the Subantarctic Zone due to a tongue of warmer (T > 16°C, yellow) Brazil Current return water, which was about to rejoin the return flow near 41°S, 52°W. Similar events are reported by *Legeckis and Gordon* [1982] and *Gordon* [1989], who note that a meander of the Brazil Current return, with amplitudes of 100–300 km, seems to from a recurrent flow pattern near 40°S, 50°W.

The disjointed structure of the cold water inclusion indicates that the density field between 39°S and 41°S (Plate 2c) should indeed be interpreted as the cyclonic feature C-γ, however, not necessarily as a coherent cold core eddy. The front between 39°S and 40°S, which was identified as BCF in the hydrographic section, must be reinterpreted as the northern frontal expression of C-γ, rather than the southernmost extension of the BCF. South of C-γ, the northwestward tongue of the Brazil Current return forms the anticyclonic meander A-α as seen in section 2.1. Owing to the lack of CTD stations between 41°S and 44.5°S, section 2.1 missed the southern boundary of the subtropical regime and the southernmost part of the BCF. This section of the BCF probably forms a common feature (the Confluence Zone proper) with the SAF, which intersects with the cruise track near 43.5°S, 54°W according to both satellite SST as well as thermosalinograph data.

3. Float Observations and Their Relation to SST Features

3.1. Float 159

The interpretation of the Confluence Zone structure in section 2.2 relates well to the trajectory of float 159 and its hydrographic data. Float 159 was launched near 39°S, 49°W (Figure 1 and Table 1), just north of the cyclonic feature C-γ as identified in section 2.2. Until November 27, 1994, the float drifted slowly southward (Plate 5, red segment) underneath SST > 16° water and near the eastern edge of a warm (SST > 18°C) meander of the Brazil Current return (Plate 1, November 18). The corresponding hydrographic properties (Plate 5b, red data) indicate a subtropical AAIW environment. The pressure and temperature records (Plates 5c–5e) are measured directly by the float, whereas density (Plate 5f) and salinity (Plate 5g) are derived under the assumption of hydrostatic equilibrium, using the known equations of state of seawater and the float [*Boebel et al.*, 1995].

After a short, nearly stagnant phase, the float moved rapidly (≈50 cm s^{-1}) from the southeastern edge of the warm water meander to the southwest. A narrow intrusion of cooler (12°C–16°C) water (Plate 1, November 28) found to the south of the warm water meander forced the Brazil Current to retroflect north of the float. The float then followed a warm water patch which apparently became detached from the retreating warm water meander (Plate 1, December 3). Meanwhile, the float shifted in temperature-salinity (TS) space toward (but not yet across) the limiting curve of the subtropical regime (Plate 5, magenta segment).

During this period, shoaling from 740 to 660 dbar (Plate 5d) is observed, which is linked to a temperature decrease (4.8°C–3.6°C, Plate 5e). This seemingly dissenting behavior is usually explained by the inability of quasi-isobaric floats to completely follow shoaling or sinking water parcels due to different compressibilities of the float and seawater [*Rossby*, 1988; *Shaw and Rossby*, 1984]. In the case of small vertical displacements of the surrounding water (for example, in internal waves), the float's (Lagrangian) θ-S data is expected to slide up/down the corresponding CTD (Eulerian) θ-S curve while it sinks/shoals relative to the surrounding water (see Appendix A). This type of behavior has been observed in many float trajectories, primarily in quiet ocean regions away from oceanic fronts [*Boebel et al.*, 1997].

However, the Lagrangian θ-S data of float 159 during early December 1994 deviates distinctly from the θ-S CTD data taken at the float launch position (Plate 5b, thin line). During a transitional phase (magenta segment) the float's θ-S data evolved from a subtropical environment (red data) to a cooler and fresher θ-S regime (green data) near the boundary between subtropical and Malvinas Current core water. The associated substantial decrease in salinity cannot be explained by a vertical displacement of the float relative to the surrounding water and concurrent adhesion to the corresponding water column, since originally the float was deployed close to the local salinity minimum.

Most likely the quasi-isobaric float failed to follow the shoaling of its surrounding water and descended into the underlying waters (see *Boebel et al.* [1995, Figure 2] for a schematic of this process) of the cooler and fresher subantarctic site of the Brazil Current Front (due to the sloped isopycnals at the BCF). Hereinafter we will use the term "migration" to describe the cross-frontal net float displacement resulting from of the combination of vertical float and water displacement (due to sloping isopycnals at oceanic fronts) and the float's opposing response (due to its lower compressibility).

A direct result of the float's migration from one side of the front to the other is the instrument's dissociation from the water parcel it originally tagged. Therefore we cannot conclude unreservedly that subtropical water was mixed across the Brazil Current Front into the subantarctic region. Instead, we observe that the substantial shoaling (order of 100 m) of subtropical AAIW led to the detachment of the float from its subtropical environment and the capture of the float by fresher and cooler water.

Reaching its southernmost position near 41.5°S on December 8, float 159 was then captured by the prevailing cyclonic circulation around the cold core feature C-γ and carried to the northwest (Plate 5, green data). This trajectory segment is located underneath surface water of subantarctic origin (Plate 1, December 8), but rather unusually, the float θ-S data indicate a subtropical float environment together with the cessation of the shoaling process (Plate 5, green data).

The subsequent fast northeastward motion along and underneath a strong SST gradient (Plate 1, December 18, SST < 18°C to SST > 20°C) at nearly 70 cm s^{-1} is linked to a first migration of the float from the subtropical to the subantarctic

environment (Plate 5, cyan data), which, however, is reversed shortly after. The corresponding 50-dbar spike in the pressure record motion is associated with rather stable temperatures.

Commencing with the cusp-like trajectory segment near 40°S, 47°W (Plate 1, December 23, and Plate 5, cyan to blue transition), which was related to a warm water (SST > 18°C) meander, the float was carried eastward in the meandering South Atlantic Current. The corresponding trajectory segment is confined to the subtropical region north of the 16°C outcrop (Plates 1 and 6). The concurrent Lagrangian θ-S data, however, which evolved into a typical Eulerian θ-S profile near the salinity minimum, suggest that the float did not trace subtropical water (Plate 5b, blue data). On the contrary, the float was retained within a parcel of fresher Confluence Zone water for a period of 6 months until early June 1995.

During this period the derived salinity decreased slightly, reaching its minimum below 34.2 in early April 1994. This is related to warming surrounding waters, as observed in the float temperature record. The higher temperature resulted in a less dense environment, which made the float sink (due to its unchanged density based on the very small coefficient of thermal expansion). The float thus slowly descended into underlying water of lower salinity.

3.2. Float 158

The transport of fresh Confluence Zone water towards the interior subtropical gyre also is confirmed by float 158 (Plate 7a). This float was launched ~1° north of float 159 into the cyclonic feature C-β at 38°S. Close examination of the float trajectory reveals a zigzag pattern that prevailed until end of January 1995 (Plate 7a, blue segment). Such a pattern indicates that the float was trapped near the center of an eddy, but owing to a daily sampling scheme, the float was unable to resolve its circular flow path. The tagged eddy must have had a rotation period of about 2 days, resulting in an estimated tangential speed of 25 cm s^{-1} at the observed radius of 7 km. The strong aliasing effect prohibits us from deducing whether the float was trapped in a cyclonic or anticyclonic circulation from the trajectory directly. A cyclonic interpretation, however, is in agreement with the hydrographic observation of a mesoscale cyclonic subsurface feature C-β, into the center of which the float was launched.

During the period of cyclonic motion the lowest salinities (≈34.17) measured by any of our floats (Plates 7b and 7g, blue data) were observed by float 158. This statement, however, is not independent of the corresponding CTD cast (Plate 7b, thin curve) since during the calculation of float salinity a renormalization is applied (Table 2) which matches the first few days' float θ-S data to the CTD data (see Appendix B). Nevertheless, the low salinity values persisted for >2 months, and the patch of subantarctic properties was traced without much alteration into the subtropical gyre interior.

Just prior to the end of the cyclonic movement, we observe a reversal of the southeastward translation which was superposed to the circular motion in late January. The subsequent cessation of the circular motion on January 28, 1995, is correlated with the observation of warmer and saltier water of 34.25 and 34.35 (Plate 7, red data). All subsequent Lagrangian θ-S data fall into the subtropical regime, reproducing the shape of Eulerian θ-S diagrams of the subtropical AAIW regime. During this time, float 158 flowed along the meandering structure formed by the boundary of the SST > 18°C water (Plate 6, March 18 and 28), apparently trapped by the South Atlantic Current. Contrary to the cross-frontal migration and associated property changes observed for float 159, the strong temperature changes in February and early November 1995 are explicable by assuming that the float adheres to a given water column and slides up and down a fixed, subtropical θ-S relation.

3.3. Float 155

On a larger scale, float 158 followed an anticyclonic arch during November and early December 1994 which resembles the trajectory of the neighboring float to the north (Plate 1), float 155. Float 155 had been seeded between the two cyclonic features C-α and C-β and left this region in an anticyclonic loop (Plate 8a), which is not unexpected for water trapped between two cyclonic features. The θ-S data of float 155 shows slight freshening into Confluence Zone properties (from S = 34.23 to 34.21, red data in Plates 8b and 8g) during this anticyclonic period, which probably can be related to mixing with water from the fresh eddy C-β to the south. In fact, float 155 approached float 158 (which rotates at about 7 km radius from the center of C-β) as close as 15 km on December 15, 1994 (Plate 1, December 18). According to the stable pressure record of float 158 (Plate 7d), eddy C-β had retained its vertical position at the time of closest encounter. At the time of closest encounter, float 155 was positioned at 27.18 σ_θ (Plate 8f), which coincides with the density level of the low salinity spike (S_{min} = 34.20) of CTD station 38, i.e., C-β (Plate 3, green curve).

On February 11 a marked transition is visible in the θ-S data of float 155 (Plate 8, blue data). The event is initiated by a sharp change in drift direction from southwestward to southeastward (Plate 8, end of red segment in February 1995) when the float approached the southernmost extend of SST > 20°C Brazil Current extension surface water (Plate 6, February 8). (Please note the general SST warming that occurred between November/December 1994 (Plate 1) and the February/March 1995 (Plate 6) due to the summer warming, which complicates the definition of the BCF by a single isotherm over the course of a year. Analogously, please note the overall similarity of the SST values between the November 1994 (Plate 1) and November 1995 (Plate 9).) Subsequently, the float trajectory is located near the 20°C outcrop and, drifting in a southeastward direction, shoaled by 70 dbar, while experiencing decreasing temperatures (from over 3.8°C to 3.2°C; Plates 8c–8e, blue data) between February 8 and 18 (Plate 8). This is interpreted as the float's migration through the BCF. The end of the subsurface migration process is correlated to an cyclonic turn in the float trajectory. This cyclonic trajectory segment marks the float crossing over the southernmost extension of >20°C surface water (Plate 6, February 18) which is deflected northwards and somewhat to the east.

Between March 18 and 28 the float drifted southwestward, finally reaching the edge of the SST > 16° regime by the end of March (Plate 6, March 28) when it is deflected eastward. Throughout May and June 1995, float 155 experienced shoaling from 820 dbar to ~700 dbar, coupled to a decreasing temperature from around 3°C to 2.8°C (Plate 8, green data). This is reflected in the θ-S diagram (Plate 8b) by a transition from the (blue) data cluster around 3° to a stretched array of (green) data with limited temperature (2.5°–2.8°) but wide salinity range (34.29–34.45). This indicates that the float continuously observed the presence of a subpolar environment. The θ-S data occupy the region between the lower limit of

interior trough properties (Plate 8b, black curve on the left) and the Malvinas Current Core water (Plate 8b, black curve in the middle), but these curves are in close proximity at densities below 27.3. A clearer classification can be made in the pressure-temperature diagram (Plate 8c), where the green float data are found on the subpolar side of the separating line between subantarctic and subpolar station data (Plate 4).

The float reached its southernmost position in late June and early July 1995, which coincides with the lowest temperatures record of 2.6°C. Thereafter, a small cyclonic eddy trapped the float [*Boebel et al.*, 1999] and transported it northward to the Brazil Current Front. The corresponding SST distributions of October 1995 (Plate 9) reveal flow patterns distinctly different from those observed a year earlier. The Brazil Current had detached from the western boundary near 34°S and the Brazil Current extension (surface water > 16°C) protruded to 43°S where it mainly retroflected to the north. A more than 100-km-wide band of cold subantarctic water (C-δ) separated a large elongated anticyclonic warm core eddy (A-β), observed at 43°S, 54°W, from the Brazil Current extension. This eddy separated the eastern branch of subantarctic water from the western main branch of the Malvinas Current return, which presumably flowed south along the eddies' (A-β) western boundary.

The small (unnamed) eddy tagged by float 155 was advected north with the anticyclonic circulation pattern along the eastern boundary of the elongated large warm core eddy A-β. Between October 8 and 18, small-scale cyclonic loops of float 155 mark the center of the cyclonic feature C-δ near 40°S, 51°W. The float's small-scale circulation was transformed into a larger-scale motion in early October 1995 (Plate 9, October 18), when the float was situated in the center of C-δ. The resulting cyclonic motion carried the float northward along the western boundary of C-δ (which presumably was located between 38°S and 40°S along 54°W, Plate 9, October 18) and then southwestward along the BCF (Plate 9, October 28).

After November 19, 1995, the instrument moved in a southward direction and experienced a drastic descend from 750 to 900 dbar between November 20 and 30, linked to a temperature increase by nearly 1.5°C, reaching 4.3°C (Plates 8c–8e, magenta). This dramatic cross-frontal migration from a subpolar via subantarctic to subtropical environment coincides with the corresponding float trajectory being finally located underneath the meander of SST > 16° water along 50°W (Plate 9, November 18 and subsequent SST data, not shown). Subsequently, the float tagged waters of subtropical properties (Plate 8b, magenta data) until it surfaced in early December 1995.

3.4. Float 150

Simultaneously with float 155, float 150 tagged the cyclonic cold core meander C-δ of the Malvinas Current return. Float 150 had been launched in the Vema Channel near 31°S, 39°W. It drifted toward and later along the Brazilian shelf (Plate 10a, red segment) until it reached 37°S on October 1, 1995. There the float departed from the western boundary (Plate 10, cyan data before October 8) and shortly experienced a subantarctic environment as evidenced by the low salinity (Plates 10b and 10g, cyan data). This indicates the float's first migration across the BCF. However, the float is reentrained in the subtropical environment while closely following the BCF (Plate 9, October 18). Flowing along the front, the float experienced further strong vertical displacements (Plate 10d, cyan data) until October 20, indicative of the floats continuous interaction with the BCF. Commencing on October 20, 1995, the last strong (130 dbar) shoaling process led to a subtropical float environment (Plate 10b, magenta data), reaching the shallowest drifting depth at less than 850 dbar in early November 1995. Within this subtropical environment the float continued to its southernmost position underneath a warm Brazil Current extension meander (Plate 9, October 28). The preceding southward float trajectory segment is possibly located along the eastern subsurface edge of C-γ, which might better be described by the SST distribution on October 18 and be masked in the October 23 and 28 SST image by ongoing surface warming.

Subsequently, the float drifted northward along the western boundary of the cold core intrusion C-δ (Plate 9, November 8), justifying the assumption of a cyclonic circulation pattern within this cold core feature. During this period the float traces subtropical water underneath a surface layer of subantarctic properties. This produces an unusual structure, indicative for interleaving of subantarctic and subtropical water and reversing the classical picture of Malvinas Current Core water descending below the South Atlantic Central Water.

The drift of float 150 changed to northeastward when the float approached the BCF. Float 150 then moved across the surface expression of the BCF between November 12 and 16 (Plate 9) near 39°S, 51°W. At the time, this is the location of the southwesternmost edge of the retroflection of SST > 18°C surface water of the Brazil Current extension. Surprisingly, the float's drift across the BCF is accompanied by its migration into water of subantarctic properties, a process that continues until November 17. Originating south of the main BCF and at about 850 dbar depth, this suggests that the tagged subtropical water parcel was flowing over an underlying layer of subantarctic properties below 900 dbar into which the float then descended. Once trapped by the subantarctic environment, float 150 remained with the low-salinity water of Confluence Zone properties (S = 34.22), while it moved away from the BCF into the subtropical region and as far north as 35°S (Plate 10, blue data).

4. Discussion

Our evidence for the cross-frontal flow of intermediate water of Confluence Zone properties lies primarily in the repeated observation of subantarctic water at intermediate depth within the subtropical regime north of the BCF. Two floats (150 and 159) show the advection of fresh Antarctic Intermediate Water of Confluence Zone properties from the suspected injection site near 40°S, 50°W into the interior subtropical gyre. Retaining their subantarctic properties, these patches moved farther into the subtropical regime with the South Atlantic Current (float 159, Plate 5, blue section) and the Brazil Return Current (float 150, Plate 10, blue section).

Further evidence for the cross frontal exchange from the subantarctic to the subtropical side of the Confluence Zone is provided by the subantarctic AAIW properties which were found near 38°S in the hydrographic section within the subtropical regime. Float 158, launched into the center of this subsurface low-salinity lens, subsequently traced the northeastward drift of this feature for 2 months from 38°S, 47°W to 36°S, 41°W (Plate 7, blue segment), while simultaneously revealing its eddy structure (C-β). Similarly, the water parcels surrounding floats 159 and 150 retained their low values of salinity for extended periods. These floats noted incremental salinity in-

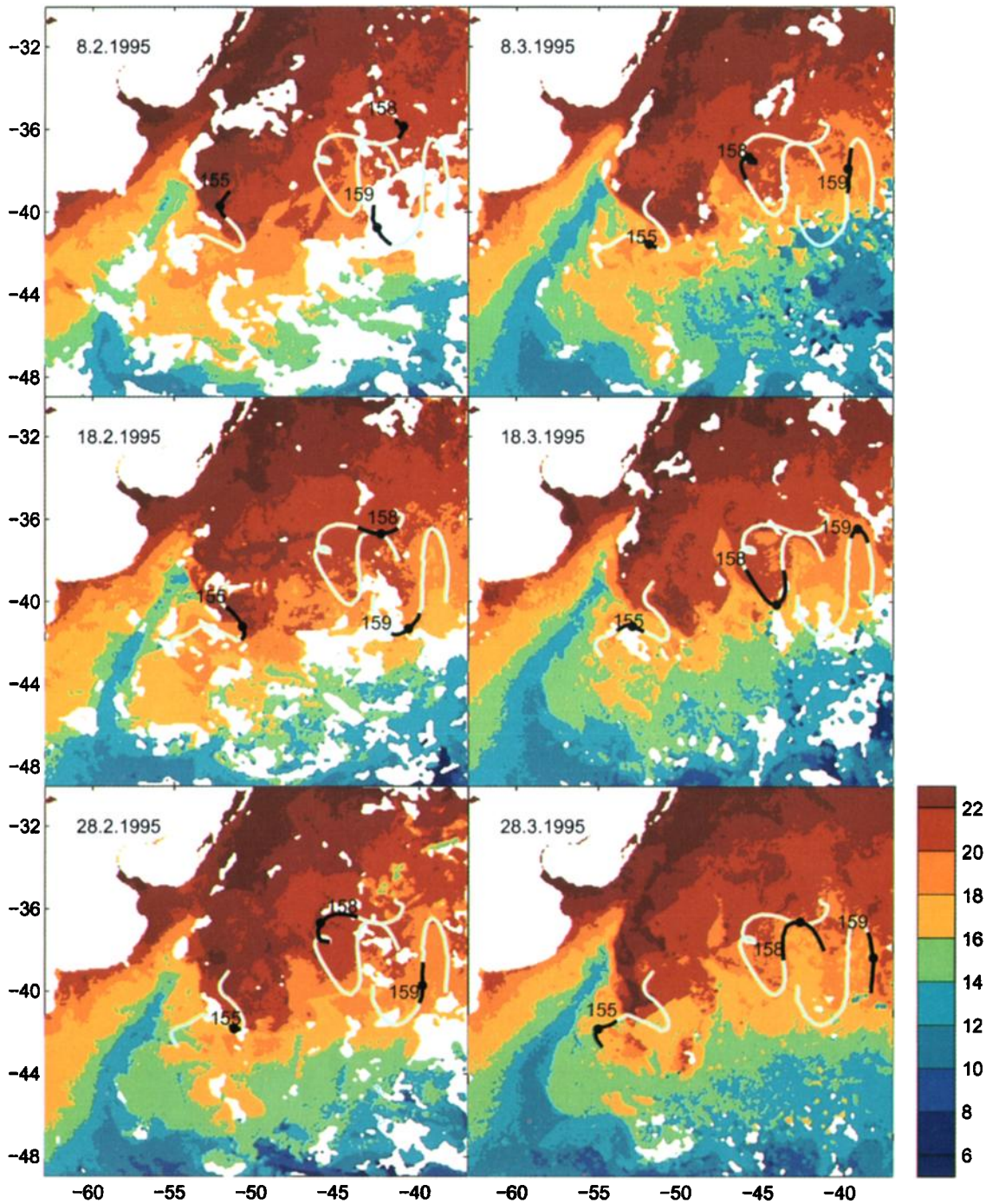

Plate 6. Satellite sea surface temperature of the Confluence Zone between February 8, 1995, and March 28, 1995. The SST images are 5-day maximum temperature composites, centered around the day indicated in the top left corner in day-month-year format. Float trajectory segments (black) spanning 10 days are centered around the same date (with the corresponding float position indicated by a dot). The float number is indicated next to the segment start. As guide to the eye, gray float trajectory segments span the total period (February 8 to March 28, 1995) covered by this figure.

Table 2. Temperature (T) and Tank Temperature (T_T) Corrections Applied When Calculating Density and Salinity From RAFOS Float Data

Float	N	ΔT,°C	ΔT_T,°C
150	2	−0.3	0.5
155	5	−0.6	0.3
158	4	−0.4	0.2
159	3	−0.2	0.2

N indicates the number of initial float data points used to calculate the given offset by matching float and corresponding CTD cast. See *Boebel et al.* [1995] for details.

creases only after 4 and 1 months, having reached 40°S, 30°W and 35°S, 44°W, respectively.

On the basis of the analysis of Confluence Zone CTD data, *Bianchi et al.* [1993] discuss the amount of heat and freshwater transfer across the Brazil-Malvinas Confluence Zone and the dissipation of patches advected across the front [*Bianchi et al.*, 1993]. For small and relatively weak intrusions of 7 km diameter and temperature and salinity anomalies of $\Delta T = 2.6$°C and $\Delta S = 0.35$, they calculated a dissipation time of 1 week. Larger eddies of order 100 km diameter with anomalies of $\Delta T = 5.3$°C and $\Delta S = 0.7$ as observed by *Gordon* [1989] were estimated to last ~6 months.

Our observations for eddy C-β which features salinity and temperature anomalies of 0.35 and 3.5°C (at the 550 dbar level) and a radius of at least 7 km indicate a lifetime of over 2 months. This is considerably longer than the estimates given by *Bianchi et al.* [1993]. Probably, the fine structure that generates the described small-scale mixing processes is weakened with time once the eddy drifts away from the frontal zone. The reported faster dissipation of heat than salt anomalies [*Bianchi et al.*, 1993], however, does support our explanation of the increasing temperatures observed by float 159 and its response by slowly sinking into less saline waters.

On a more speculative basis the float trajectories point toward the reoccurring cold core meander near 40°S, 50°W as the preferred site cross-frontal exchange. The three floats (150, 155, and 159) that experienced cross-frontal migration from the subtropical to the subantarctic side or vice versa did so in close vicinity of this frequently observed cold core feature (Table 3). Subsequently, two of these floats (159 and 150) returned to the subtropical gyre interior but traced subantarctic water patches rather than a subtropical environment.

We have given a detailed description on how cross-frontal float migration is in part due to the quasi-isobaric character of the floats. Nevertheless, the floats cross-frontal velocity component reflects similar vertical and lateral (with respect to the frontal axis) flow patterns of the surrounding water, which are likely to produce interleaving of warm, saline and cold, fresh water. Such structures were observed here directly at CTD station 41 (Plate 3, cyan) or indirectly in the unusual situations encountered by floats 150 and 155, i.e., the observation of a subtropical environment at intermediate depth with subantarctic water at shallower depths.

Similar interleaving structures of density compensating warm, saline and cold, fresh water are considered to be important for cross frontal transport of intermediate water in the Crozet Basin [*Park and Gamberoni*, 1997]. At the 1200-dbar level, near the combined subtropical and subantarctic frontal region, they observed salinity anomalies of $\Delta S = 0.23$, which is of similar magnitude at the anomaly observed here at C-β. In the Crozet Basin, repeated CTD stations at a fixed position revealed the impulsive injection of fresh intermediate water from the subantarctic to the subtropical side, associated with an interleaving thermal and haline structure [*Park and Gamberoni*, 1997]. The injections did occur in particular below the $27.1\sigma_\theta$ density surface and in a nonuniform manner along the underlying density surfaces. Also, injections were not continuous in time and space, similar to the observations made here, where (1) extended periods of relative stability of the Lagrangian θ-S data along frontal SST features suggest the unlikeliness of cross-frontal exchange but (2) the observation of low-salinity patches north of the front necessitates the sporadic existence of such exchange processes.

In addition to the findings by *Park and Gamberoni* [1997] our Lagrangian method enables us to trace the subantarctic intrusions farther into the subtropical regime. The float trajectories, when tracing a low-salinity feature, thus illustrate possible connecting routes between isolated lenses (e.g., C-β and the lens at stations 16 and 18 in Figure 3 of *Park and Gamberoni* [1997]) and the corresponding injection site (e.g., as indicated by station 41, cyan curve in Plate 3 or by Figure 12 of *Park and Gamberoni* [1997]) as observed in hydrographic studies.

When subtropical to subantarctic cross-frontal float migration occurred, it was linked to a cyclonic float trajectory segment associated with an anticyclonic bend in the BCF. In two instances, when the respective float was trapped by the Brazil Current extension (floats 155 and 159), our findings bear some similarity to observations made by *Bower and Rossby* [1989] in the North Atlantic Gulf Steam. Using isopycnal RAFOS floats, they discovered that Gulf Stream meanders contribute significantly to the loss of water from the stream and that losses occurred primarily upstream of meander crests or troughs [*Song and Rossby*, 1995]. On the northern side of the Gulf Stream, anticyclonic flow and upward sloping isopleths (as viewed from the center of the stream) characterize a meander crest.

A mirror picture can be found in the Brazil Current extension when it retroflects to the north at its southernmost extensions. Analogously, Gulf Stream troughs, which are associated with cyclonic flow and descending isopleths, are comparable to troughs of the Malvinas Current return meanders. *Bower and Rossby* [1989] report that the observed losses of floats from the stream are highly correlated with significant shoaling (sinking) of the floats while the flow approached the crest's (trough's) extreme. Our limited data are obviously not as conclusive as the analysis by *Song and Rossby* [1997], but nevertheless, our findings do show a similar correlation and give first hints that the exchange of AAIW might occur at regions upstream of strong curvature segments of the Brazil Current Front and in connection with significant vertical displacements.

On the basis of the same data as the *Bower and Rossby* [1989] and *Song and Rossby* [1997] studies, *Bower and Lozier* [1994] conclude that most of the observed particle exchange between the Gulf Stream and its surrounding waters is not representative of cross-frontal exchange. *Bower and Lozier* [1994] find a strongly reduced cross-frontal property exchange at (shallow) density levels where a strong potential vorticity front exists, whereas at deeper levels, where strong particle exchange does indeed occur, the waters are relatively homogenous on both sides of the dynamical boundary formed by the deep reaching Gulf Stream. In the Crozet Basin, *Park and Gamberoni* [1997] observe that the combined subantarctic and subtropical frontal

Table 3. Float Migrations Across the Brazil Current Front

Float	Date	Position	SST Feature
159	Nov. 28 to Dec. 4, 1994, magenta segment	40°S, 49°W	southwestern edge of SST > 18°C/20°C BCF
155	Feb. 10–18, 1995, first part of blue segment	41°S, 51°W	southernmost edge of SST > 20°C/22°C BCF
150	Nov. 11–18, 1995, magenta to blue transition	39°S, 51°W	southwesternmost corner of SST > 18°C BCF meander

zone also acts as an effective dynamical barrier for waters lighter than 27.1, but not below, due to the absence of a vorticity front at these greater depths. However, different from the situation in the Gulf Stream, particle exchange in the intermediate layers of the Crozet Basin and the Brazil-Malvinas Confluence Zone does represent significant property fluxes due to the strong property gradient present there in the 27.0 to 27.3σ_θ layer (Plate 3). Hence the conclusion by *Bower and Lozier* [1994] that at greater depth, cross-frontal processes are absent in the Gulf Stream due to the lack of a property front does not apply here.

Appendix A: Interpretation of Lagrangian θ-S Data

The rigorous interpretation of individual three-dimensional trajectories of quasi-isobaric floats in terms of the motion of the tagged water parcel is restricted by the lack of knowledge of the represented water type at a given time. Pressure and temperature records, which are the standard quantities measured by RAFOS floats, provide only incomplete information on the float's environment. The calculation of salinity under the assumption of hydrostatic equilibrium does under most circumstances resolve this shortcoming by making the float data suitable for traditional watermass analysis in potential temperature-salinity diagrams. The concept of θ-S diagrams has proven of great usefulness for the description of the ocean since water types can easily be distinguished regardless of their depth. The most simple Lagrangian θ-S diagram would be a single point in θ-S space. This means that the physical properties of a given water parcel are conserved while it follows its three-dimensional trajectory. Under the absence of mixing, the motion of a water parcel along an isopycnal surface does leave no trace in the θ-S diagram, and hence isopycnal floats [*Rossby et al.*, 1985] should also show only single points in θ-S space while drifting within an unaltered environment.

In this study, however, we used quasi-isobaric floats, i.e., floats that have a considerable (by a factor of 10) lower compressibility than the surrounding seawater, rendering the float unable to follow shoaling or sinking water parcels completely. As a result, anticorrelated pressure and temperature records are frequently seen in the float data, making a quantitative interpretation of the float's motion relative to its environment difficult. When, however, a CTD station of the water column into which the float was originally set is available and the composition of the tagged water remained unchanged during the time of mutual drift, the cloud of Lagrangian θ-S data should match the corresponding CTD θ-S relation. This is because relative vertical displacements between the float and its original environment result in the float θ-S data sliding up and down along the given Eulerian (CTD) θ-S relation. The reverse conclusion is applicable as well: a match between Eulerian and Lagrangian θ-S data indicates the coupling of the float and its original environment and the conservation of the physical properties of the latter.

Deviations between the float θ-S data and CTD θ-S relation on the other hand indicate mixing processes (isopycnal or diapycnal) and/or the float's self-induced migration into waters of different θ-S properties. So far, it is difficult to distinguish between mixing and migration-induced deviations with our isobaric floats, but the rapidity with which changes occurred favors migration over mixing. The use of isopycnal floats in future studies should omit migration almost entirely and should thus provide a direct view of the path of a given water parcel and the evolution of its hydrographic environment.

Appendix B: Errors in Derived Salinity Data

The conclusions presented above do in part rely on float salinities, which are derived from RAFOS float pressure and temperature records under the assumption of hydrostatic equilibrium. The method and associated errors have been described by *Boebel et al.* [1995]. Since then, a number of technical improvements have been achieved, and long-term pressure sensor stability measurements were performed, which improve the error estimates given by Boebel et al.

When calculating the float salinity, renormalization of the float temperature calibration and of its density has to be applied [*Boebel et al.*, 1995]. Early problems with the float temperature calibration have meanwhile been investigated and resolved but unfortunately only after the deployment of the floats used in this study. The reason for the miscalibration was that the float temperature circuit is an AC circuit, where the impedance of the thermistor modifies the resonance frequency. When the thermistor was replaced by a resistance decade during the calibration procedure, a false impedance was introduced to the circuit, which resulted in slightly altered calibration data.

At the time of developing this method of salinity calculation the need for an adjustment of the float density was traced to the mismeasurement of the pressure tank temperature while the floats were ballasted. Parallel to the built-in temperature sensor, which proved to be rather unstable, we now use a high-precision SIS reversing thermometer at three different tank depths in order to verify the temperature measurement and to monitor the developing temperature stratification within the tank. Using the reading from the reversing thermometer and mixing the tank thoroughly in case of stratification resulted in a much better agreement between the prelaunch float density determination, based on the corresponding CTD cast, and the postmission determination from the float data. We now have to apply tank temperature corrections of the order of 0.3°C (Table 2), whereas >1°C were necessary when this method was first used [*Boebel et al.*, 1995].

The generation of floats used by *Boebel et al.* [1995] observed a bimodal distribution of pressure and temperature data at a fixed pressure or temperature. This problem, which essentially limited the precision of these measurements to ±10 dbar and ±0.1°C, was resolved through the use of a modern float board design provided by Bathy Systems. The new errors estimates

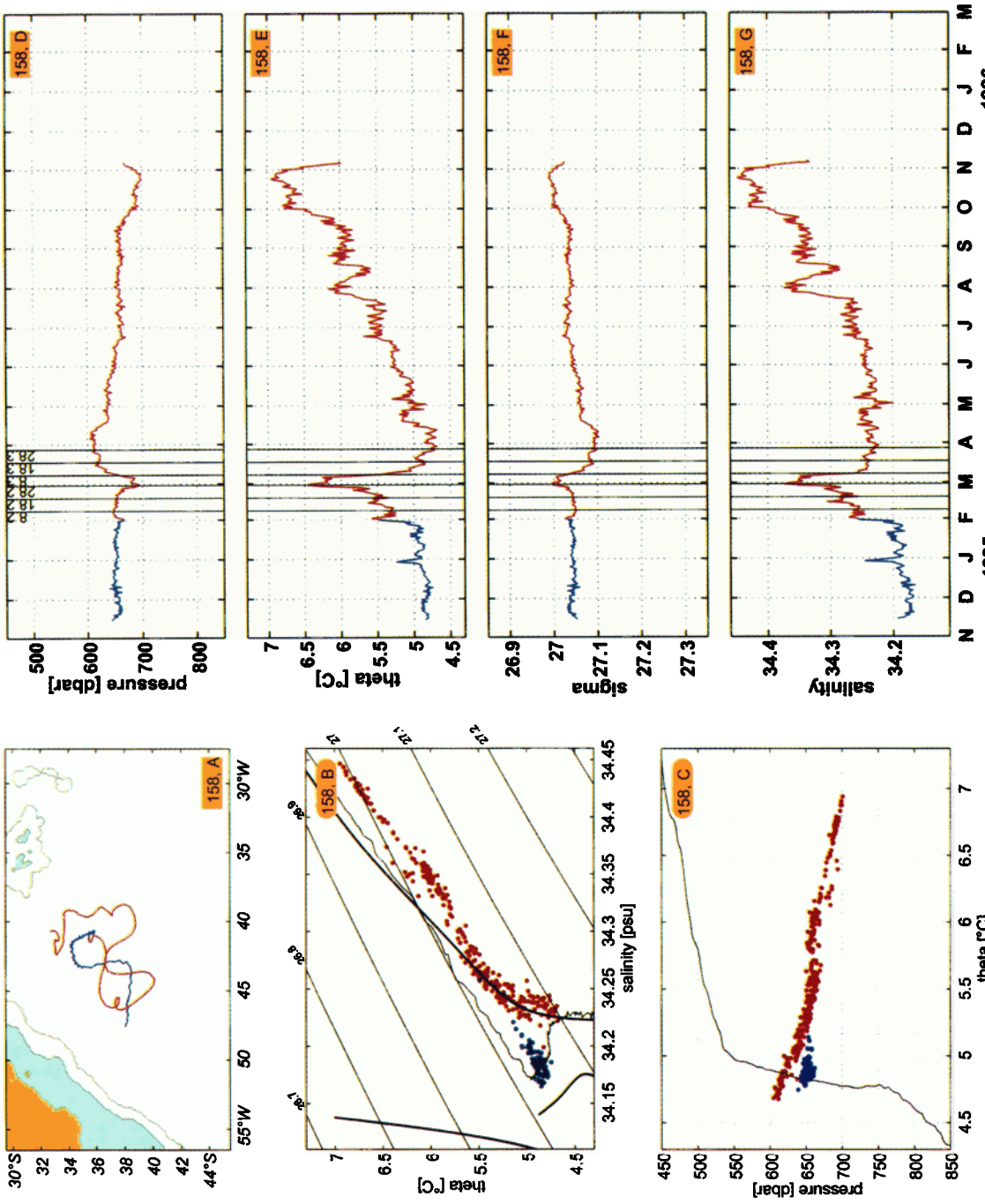

Plate 7. Float 158. (a) Full trajectory between launch and surface position. The float surfaced on schedule after nominal 12 months. (b) Lagrangian potential temperature-salinity diagram (dots). The boundaries between different water regimes are given as curves (compare Plate 3). The CTD cast taken prior to the float seeding is depicted as thin curve. (c) Pressure-potential temperature diagram. (d) Pressure, (e) potential temperature, (f) potential density, and (g) salinity time series. Vertical lines refer to times at which satellite images are discussed (Plate 6).

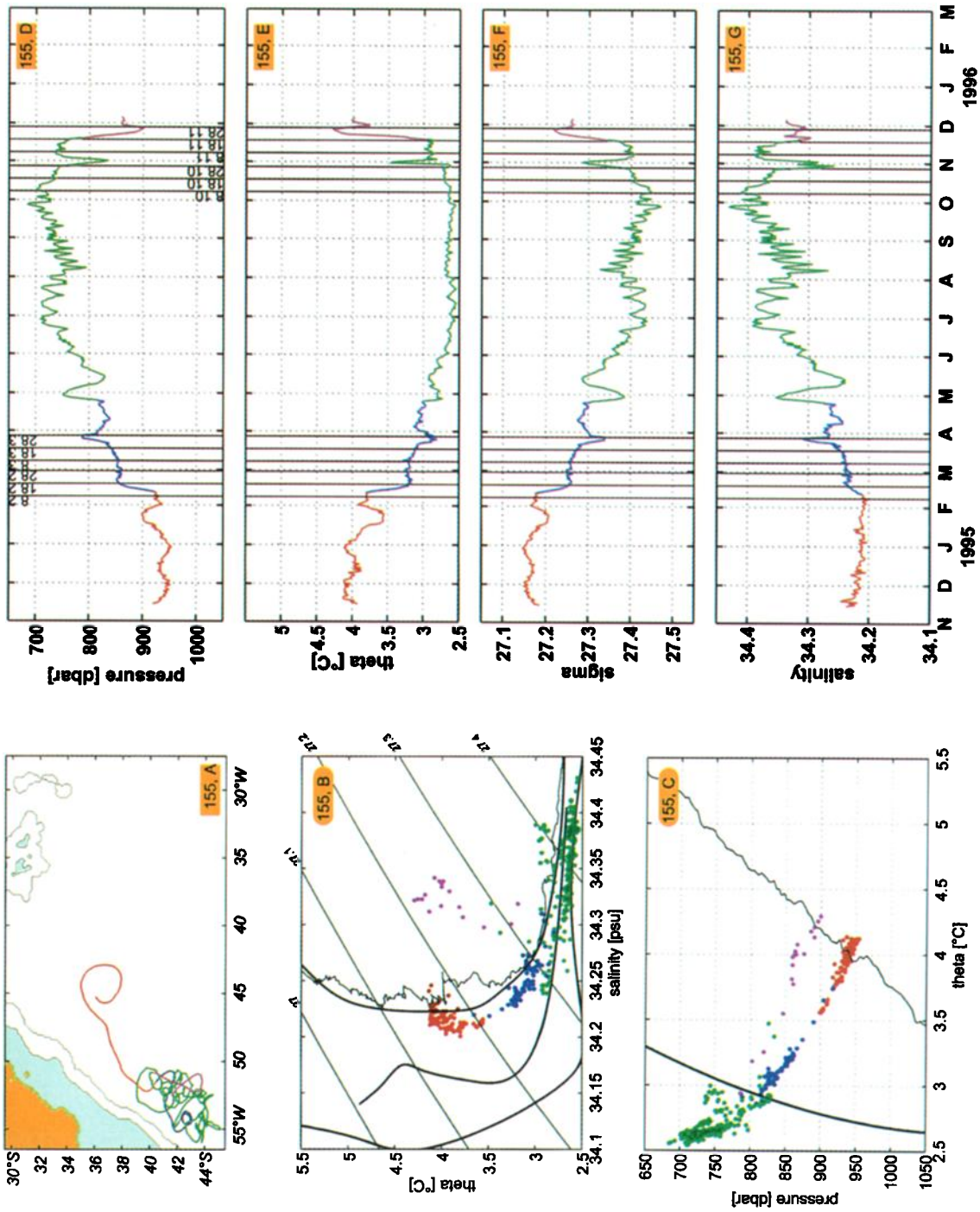

Plate 8. Float 155. (a) Full trajectory between launch and surface position. The float surfaced on schedule after nominal 13 months. (b) Lagrangian potential temperature-salinity diagram (dots). The boundaries between different water regimes are given as solid curves (compare Plate 3). The CTD cast taken prior to the float seeding is depicted as thin curve. (c) Pressure-potential temperature diagram. (d) Pressure, (e) potential temperature, (f) potential density, and (g) salinity time series. Vertical lines refer to times at which satellite images are discussed (Plates 6 and 9).

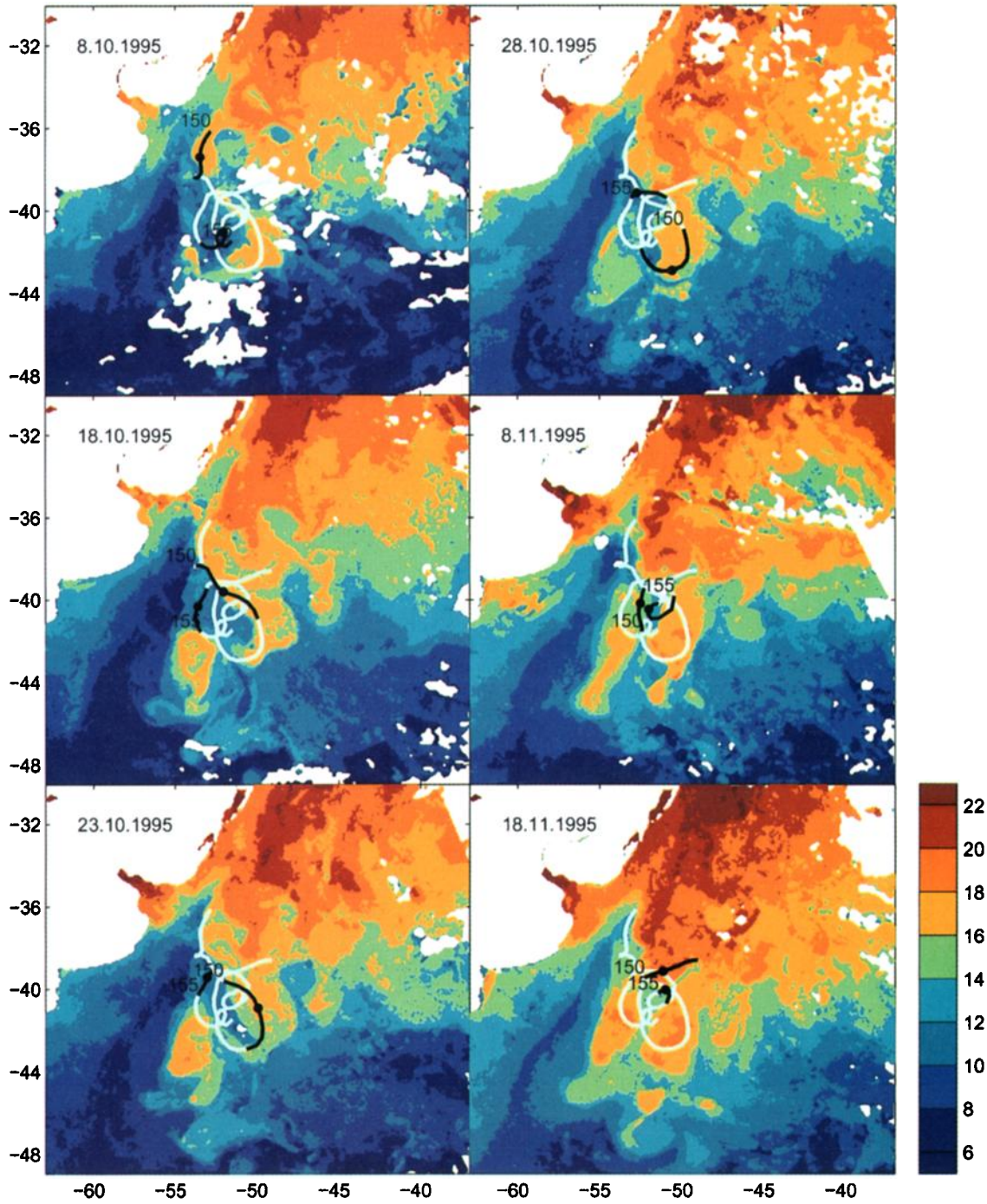

Plate 9. Satellite sea surface temperature of the Confluence Zone between October 8, 1995, and November 18, 1995. The SST images are 5-day maximum temperature composites, centered around the day indicated in the upper left corner in day-month-year format. Float trajectory segments (black) spanning 10 days are centered around the same date (with the corresponding float position indicated by a dot). The float number is indicated next to the segment start. As guide to the eye, gray float trajectory segments span the total period (October 8 to November 18, 1995) covered by this figure.

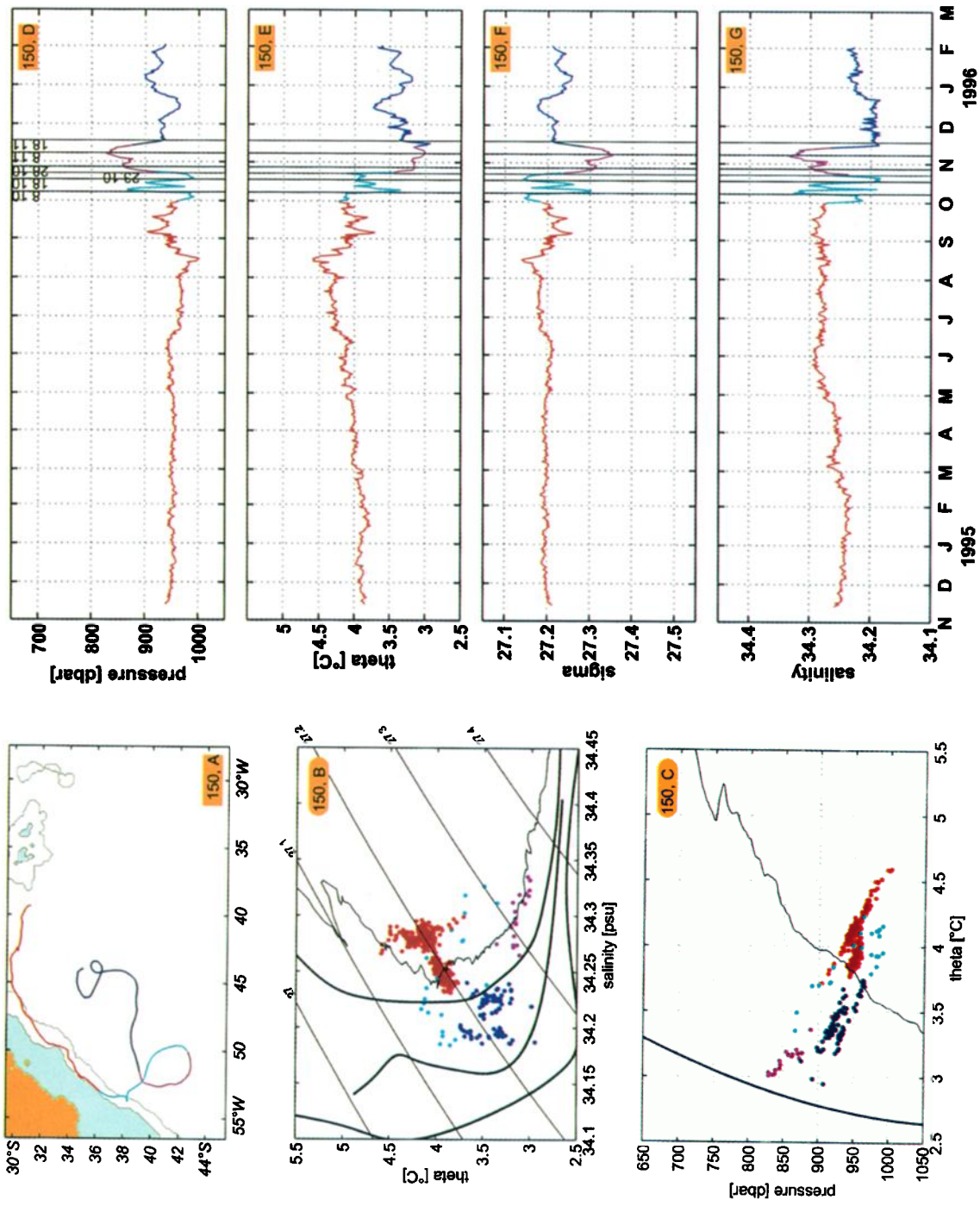

Plate 10. Float 150. (a) Full trajectory between launch and surface position. The float surfaced on schedule after nominal 15 months. (b) Lagrangian potential temperature-salinity diagram (dots). The boundaries between different water regimes are given as curves (compare Plate 3). The CTD cast taken prior to the float seeding is depicted as thin curve. (c) Pressure-potential temperature diagram. (d) Pressure, (e) potential temperature, (f) potential density, and (g) salinity time series. Vertical lines refer to times at which satellite images are discussed (Plate 9).

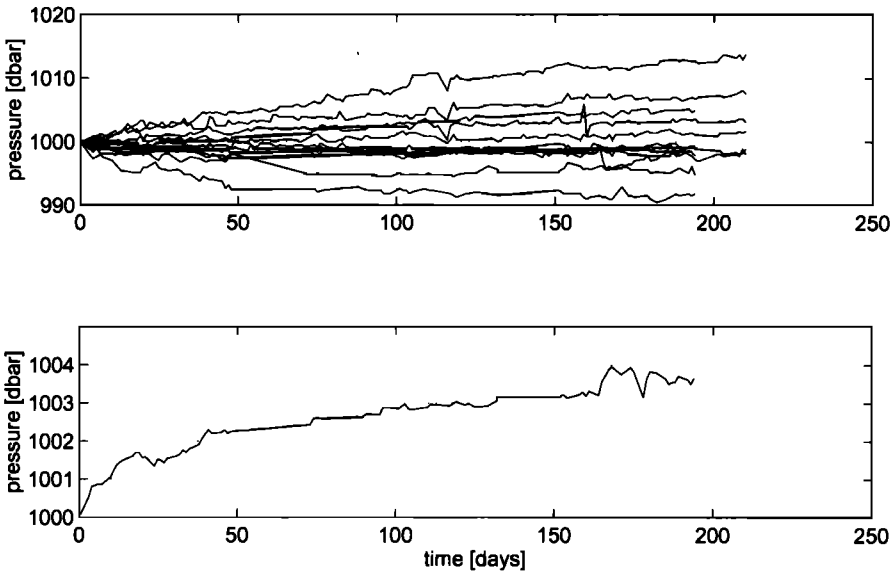

Figure 3. (top) Normalized pressure output of 12 pressure sensors, held at 1000 dbar for up to 7 months. (bottom) Mean absolute pressure deviation from 1000 dbar for the above sensors.

are considerably smaller (±0.02°C and ±2 dbar). This in turn improves the estimated precision for the salinity calculation to 0.005 psu, a quarter of the value quoted previously.

Of greater concern is the long-term stability of the pressure sensor as well as the float's pressure housing, a glass tube in combination with a stainless steel endplate. The pressure sensor stability was investigated in the laboratory (Figure 3, top), by initially exposing six sensors for 210 days to a pressure of 1000 dbar. Daily pressure measurements were taken and recorded. Two of these pressure sensors showed notable creep of order 10 dbar within the period of observation. We then decided to replace the four sensors that showed little creep with new samples and to continue the experiment. The new batch confirmed the earlier result of some sensors creeping notably, while others showed nearly no creep at all.

The analysis of the data in form of the mean absolute pressure deviation from 1000 dbar (Figure 3, bottom) shows the roughly exponential behavior of the pressure drift. The timescale is of the order of 20 days and is probably valid for all sensors, but the magnitude is obviously of no relevance because of the strong intersensor differences. The maximum error to be expected from the pressure sensor drift is about 18 dbar yr^{-1}, or, in terms of salinity miscalculation, 0.025 psu. The result suggests that the performance of the pressure sensors can be improved significantly by prestraining the sensors in the laboratory after they have been mounted to the float end plate.

Unfortunately, not much progress has been made with regard to the determination of the long-term stability (or creep) of the glass housing. Owing to the lack of funds and personnel we were unable to carry out a 1–2 year test in a 100-bar pressure tank or to become involved in theoretical studies of the issue of glass creep. Recent order of 2 years float records from quiescent regions of the subequatorial South Atlantic [*Boebel et al.*, 1999] indicate that errors due to glass creep can be expected to be of the same order or smaller than the errors due to the pressure sensor drift. Nevertheless, we hope to be able to pursue this matter in future, thorough investigations.

Acknowledgments. We would like to acknowledge the excellent work of officers and crew of R/V *Polarstern*. The fine workmanship of the IfM Kiel electronic and mechanic laboratories in the preparation of the floats is highly valued. An extensive and detailed discussion with Alberto Piola on the Confluence Zone during the Brest WOCE Workshop was particularly helpful in the preparation of this work. Similarly, the critical but constructive remarks of two unknown reviewers helped to significantly improve the manuscript. The project benefited substantially from the ongoing cooperation with the Alfred Wegener-Institut, Bremerhaven, and was financed by the German Bundesministerium für Bildung, Forschung und Technologie. The AVHRR data were collected at Estación HRPT en Alta Resolución (Buenos Aires, Argentina) by Servicio Meteorológico Nacional, as part of a cooperative study with the University of Miami. Olaf Boebel acknowledges his current support through the Alexander von Humboldt Foundation. This paper is dedicated to Uwe Huenninghaus, who has built over 230 RAFOS floats at the IfM-Kiel and who now attends his well-deserved retirement.

References

Bianchi, A. A., C. F. Giulivi, and A. R. Piola, Mixing in the Brazil-Malvinas Confluence, *Deep Sea Res., Part I, 40*, 1345–1358, 1993.

Boebel, O., and C. Schmid, RAFOS floats in the South Atlantic, in *Berichte zur Polarforschung*, pp. 6–11, Alfred-Wegener Inst. fur Polar- und Meeresforsch., Bremerhaven, Germany, 1995.

Boebel, O., K. Schultz Tokos, and W. Zenk, Calculation of salinity from neutrally buoyant RAFOS floats, *J. Atmos. Oceanic Technol., 12*, 923–934, 1995.

Boebel, O., C. Schmid, and W. Zenk, Flow and recirculation of Antarctic Intermediate Water across the Rio Grande Rise, *J. Geophys. Res., 102*(C9), 20,967–20,986, 1997.

Boebel, O., C. Schmid, and W. Zenk, Kinematic elements of Antarctic Intermediate Water spreading in the western South Atlantic, *Deep Sea Res., Part II, 46*, 355–392, 1999.

Bower, A. S., and S. M. Lozier, A closer look at particle exchange in the Gulf Stream, *J. Phys. Oceanogr., 24*, 1399–1418, 1994.

Bower, A. S., and T. H. Rossby, Evidence of cross frontal exchange processes in the Gulf Stream based on isopycnal RAFOS float data, *J. Phys. Oceanogr., 19*, 1177–1190, 1989.

Confluence Principal Investigators, Confluence 1988–1990: An intensive study of the southwestern Atlantic, *Eos Trans. AGU, 71*, 1131–1133, 1137, 1990.

Davis, R. E., D. C. Webb, L. A. Regier, and J. Dufour, The Autono-

mous Lagrangian Circulation Explorer, *J. Atmos. Oceanic Technol.*, *9*, 264–285, 1992.

Davis, R. E., P. D. Killworth, and J. R. Blundell, Comparison of autonomous Lagrangian circulation explorer and fine resolution Antarctic model results in the South Atlantic, *J. Geophys. Res.*, *101*(C1), 855–884, 1996.

Deacon, G. R. E., A general account of the hydrology of the South Atlantic Ocean, *Discovery Rep.*, *7*, 171–238, 1933.

Garzoli, S. L., Geostrophic velocity and transport variability in the Brazil-Malvinas Confluence, *Deep Sea Res., Part I*, *40*, 1379–1403, 1993.

Garzoli, S. L., and C. Giulivi, What forces the variability of the South Western Atlantic Boundary Currents?, *Deep Sea Res., Part I*, *41*, 1527–1550, 1994.

Garzoli, S. L., and Z. Garraffo, Transports, frontal motions and eddies at the Brazil-Malvinas Currents Confluence, *Deep Sea Res., Part A*, *36*, 681–703, 1989.

Gordon, A. L., South Atlantic thermocline ventilation, *Deep Sea Res., Part A*, *28*, 1239–1264, 1981.

Gordon, A. L., Brazil-Malvinas confluence—1984, *Deep Sea Res., Part A*, *36*, 359–384, 1989.

Gordon, A. L., and C. L. Greengrove, Geostrophic calculations of the Brazil-Falkland confluence, *Deep Sea Res., Part A*, *33*, 573–585, 1986.

Gordon, A. L., and E. Molinelli, *Southern Ocean Atlas: Thermohaline and Chemical Distributions*, 233 pp., Columbia Univ. Press, New York, 1982.

Ikeda, Y., G. Siedler, and M. Zwierz, On the variability of the southern ocean front locations between southern Brazil and the Antarctic Peninsula, *J. Geophys. Res.*, *94*(C4), 4757–4762, 1989.

Legeckis, R., and A. L. Gordon, Satellite observations of the Brazil and Falkland currents—1975 to 1976 and 1978, *Deep Sea Res., Part A*, *29*, 375–401, 1982.

Maamaatuaiahutapu, K., V. C. Garçon, C. Provost, M. Boulahdid, and A. A. Bianchi, Spring and winter water mass composition in the Brazil-Malvinas Confluence, *J. Mar. Res.*, *52*, 397–426, 1994.

McCartney, M. S., Subantarctic Mode Water, in *A Voyage of DISCOVERY, George Deacon Anniversary Volume*, edited by M. Angel, pp. 103–119, Pergamon, Tarrytown, N. Y., 1977.

Müller, T. J., Y. Ikeda, N. Zangenberg, and L. Nonato, Direct measurements of western boundary currents off Brazil between 20°S and 28°S, *J. Geophys. Res.*, *103*(C3), 5429–5437, 1998.

Olson, D. B., G. P. Podestá, R. H. Evans, and O. B. Brown, Temporal variations in the separation of the Brazil and Malvinas Currents, *Deep Sea Res., Part A*, *35*, 1971–1990, 1988.

Park, Y.-H., and L. Gamberoni, Cross-frontal exchange of Antarctic Intermediate Water and Antarctic Bottom Water in the Crozet Basin, *Deep Sea Res., Part II*, *44*, 963–986, 1997.

Peterson, R. G., On the volume transport in the South Atlantic Ocean, *Eos Trans. AGU*, *71*, 542, 1990.

Peterson, R. G., The boundary currents in the western Argentine Basin, *Deep Sea Res., Part A*, *39*, 623–644, 1992.

Peterson, R. G., and L. Stramma, Upper-level circulation in the South Atlantic Ocean, *Prog. Oceanogr.*, *26*, 1–73, 1991.

Peterson, R. G., and T. Whitworth III, The Subantarctic and Polar Fronts in relation to deep water masses through the southwestern Atlantic, *J. Geophys. Res.*, *94*(C8), 10,817–10,838, 1989.

Peterson, R. G., C. S. Johnson, W. Krauss, and R. E. Davis, Lagrangian Measurements in the Malvinas Current, in *The South Atlantic: Present and Past Circulation*, edited by G. Wefer et al., pp. 122–162, Springer-Verlag, New York, 1996.

Piola, A. R., and A. A. Bianchi, Geostrophic mass transport at the Brazil/Malvinas Confluence, *Eos Trans. AGU*, *71*, 542, 1990.

Piola, A. R., and A. L. Gordon, Intermediate waters in the southwest South Atlantic, *Deep Sea Res., Part A*, *36*, 1–16, 1989.

Podestá, G. P., B. Brown, and R. H. Evans, The annual cycle of satellite derived sea surface temperature in the southwestern Atlantic, *J. Climatol.*, *4*, 457–467, 1991.

Provost, C., O. Garcia, and V. Garçon, Analysis of satellite sea surface temperature time series in the Brazil-Malvinas Current Confluence region: Dominance of the annual and semiannual periods, *J. Geophys. Res.*, *97*(C11), 17,841–17,858, 1992.

Roden, G. I., Thermohaline fronts and baroclinic flow in the Argentine Basin during the austral spring of 1984, *J. Geophys. Res.*, *91*(C4), 5075–5093, 1986.

Rossby, H. T., E. R. Levine, and D. N. Connors, The isopycnal Swallow Float—A simple device for tracking water parcels in the ocean, *Prog. Oceanogr.*, *14*, 511–525, 1985.

Rossby, T., Five drifters in a Mediterranean salt lens, *Deep Sea Res., Part A*, *35*, 1653–1663, 1988.

Rossby, T., The North Atlantic Current and surrounding waters: At the crossroads, *Rev. Geophys.*, *34*(4), 463–481, 1996.

Rossby, T., D. Dorson, and J. Fontaine, The RAFOS system, *J. Atmos. Oceanic Technol.*, *3*, 672–679, 1986.

Schmid, C., Die Zirkulation des Antarktischen Zwischenwassers im Sudatlantik, Ph.D. thesis, Univ. of Kiel, Kiel, Germany, 1998.

Shaw, P. T., and H. T. Rossby, Towards a Lagrangian description of the Gulf Stream, *J. Phys. Oceanogr.*, *14*, 528–540, 1984.

Song, T., and T. Rossby, Lagrangian studies of fluid exchange between the Gulf Steam and surrounding waters, *J. Phys. Oceanogr.*, *25*, 46–63, 1995.

Song, T., and T. Rossby, Analysis of Lagrangian potential vorticity balance and lateral displacement of water parcels in Gulf Stream menders, *J. Phys. Oceanogr.*, *27*, 325–339, 1997.

Stramma, L., and R. Peterson, The South Atlantic Current, *J. Phys. Oceanogr.*, *20*, 846–859, 1990.

Wüst, G., Schichtung und Zirkulation des Atlantischen Ozeans, Die Stratophäre, in *Wissenschaftliche Ergebnisse der Deutschen Atlantischen Expedition auf dem Forschungs-und Vermessungsschiff "Meteor" 1925–1927*, vol. 6, pp. 109–288, Walter de Gruyter, Berlin, 1935.

Zemba, J. C., and M. S. McCartney, Transport of the Brazil Current: It's bigger than we thought, *Eos Trans. AGU*, *69*, 1237, 1988.

O. Boebel, Department of Oceanography, University of Cape Town, Private Bag, 7701 Rondebosch, South Africa. (oboebel@physci.uct.ac.za)

G. Podestá, Rosenstiel School of Marine and Atmospheric Sciences, University of Miami, Miami, FL.

C. Schmid and W. Zenk, Institut für Meereskunde, Universität Kiel, Düsternbrooker Weg 20, 24105 Kiel, Germany.

(Received June 5, 1998; revised February 9, 1999;
accepted February 25, 1999.)